Chapter 5. The Future and Recovery

Convening Lead Author: Malcolm Ko, NASA

Lead Authors: John Daniel, NOAA; Jay Herman, NASA; Paul Newman, NASA; V. Ramaswamy, NOAA

KEY ISSUES

This chapter presents results on how future halogen loading will affect the expected future behavior of total column ozone and the prospect for the detection/validation of the expected recovery trend. In a hypothetical argument, if circulation, climate and the background atmosphere were to remain unchanged as of the present-day, the projection of ozone could be based essentially upon future halogen loading. The reality though is that the concentrations of trace gases (*e.g.*, methane, nitrous oxides, and water vapor) in the atmosphere are changing because of changes in emissions, and changes in climate. The model simulated results show that the ozone increase expected between now and 2025 is largely due to the anticipated decrease in halogen loading, and ODSs will remain one of the drivers of human-caused ozone depletion up until the middle of the 21st century, when the halogen loading is expected to approach its 1980 value. Reductions in emissions of these chemicals represent the only known acceptable method to reduce this depletion in this period. The effects of climate change (largely driven by increases in CO_2) and changes in other trace gases (*e.g.*, methane, nitrous oxide, and hydrofluorocarbons) will play an increasing role in the ozone behavior. Ozone is only one

of many factors that affect UV at the surface. Future changes in UV will be discussed in this Chapter in the context of the projected ozone change in the stratosphere. The equivalent effective stratospheric chlorine (EESC) is used to compare the relative impacts of various ODS emission scenarios on future ozone. Included in this discussion is the radiative forcing associated with the halocarbons as well as the HFCs used as replacements for the ODSs. The contribution from the United States to the future halocarbon loading will be addressed in the context of EESC and radiative forcing.

The key issues, in the form of questions, that are addressed in this chapter include:

- What is the future behavior of ozone as predicted by numerical models?
- What is the future behavior of ultra-violet radiation at the Earth's surface?
- Are there any new finding concerning projected future emissions of ODSs?
- What is the radiative forcing associated with ODSs and HFCs emitted as replacement chemicals for the ODSs?
- To the extent that the emissions from a specific country can be used to estimate its contribution to global ozone depletion and radiative, what is the United States' contribution?

KEY FINDINGS

Two-dimensional chemistry transport models (both with and without climate feedback) and thee-dimensional climate chemistry models (3-D CCMs) were used to simulate the behavior of ozone in the 21st Century using projected halocarbon emissions from the WMO (2003) baseline scenario.

Analyses of simulation results indicate that:

- The halogen loading derived from prescribed surface concentrations of halocarbons in the WMO (2003) baseline scenario is estimated to recover to the 1980 value between 2040 and 2050 for midlatitudes, and between 2060 and 2070 for the polar regions.
- For the model simulated ozone content between 60N and 60S:
    - Between now and 2020, the simulated total ozone content will increase in response to decrease in halogen loading.
    - Some 3-D CCMs predict that stratospheric cooling and changes in circulations associated with greenhouse gas emissions will enable global ozone to return to its 1980 value up to 15 years earlier than the halogen recovery date.
    - Based on the assumed scenario for the greenhouse gases (which include CH_4 and N_2O), the ozone content between 60N and 60S is expected to be 2% above the 1980 values by 2100. Values at midlatitudes could be as much as 5% higher.
- For the model simulated Antarctic ozone:
    - The recovery date (the year when ozone returns to its 1980 value) for Antarctic ozone behavior depends on the diagnostics chosen. The minimum ozone value is projected not to start increasing until after 2010 in several models, while decrease in ozone mass deficit in most models has occurred by 2005.

- Model simulations show that ozone amount in the Antarctic will reach the 1980 values 10 to 20 years earlier than the 2060 to 2070 time frame.

- For the model simulated Artic ozone:
  - Ozone in the Arctic region is expected to increase. Because of large interannual variability, the simulated results do not show a smooth monotonic recovery. The dates of the minimum ozone from different models occur between 1997 and 2015.
  - Most CCMs show ozone values at 2050 larger than the 1980 values, with the recovery date between 2020 and 2040.
  - Results from the majority of the models indicate that Arctic ozone depletion will not be significantly worse than what has occurred.

With the current scenarios, anthropogenic halogens identified in the Montreal Protocol should have a negligible effect on ozone beyond 2050. In order to predict the future trend of ozone in that time frame, one must consider projections for climate changes and changes in trace gases such as other halogens, CH_4 and N_2O.

Current analyses techniques should enable one to confirm the time when halogen loading returns to its 1980 value and their influence on global ozone is minimal within five to ten years after it occurs.

The future UV trend at the surface is likely to be more dominated by changes in cloud, aerosols, and tropospheric air quality. Equivalent Effective Stratospheric Chlorine

(EESC) will still be a useful predictor for the relative effects of ODSs on future UV in terms of evaluating the different scenarios.

Equivalent Effective Stratospheric Chlorine (EESC) is a useful index for comparing relative merits of different emission scenarios in minimizing ozone depletion. Current scenario includes emissions of long-lived ODSs only and does not include projection for future emissions of very short-lived source gases.

- EESC is a useful proxy for comparing the relative impacts of various ODS emission scenarios on future ozone. The absolute timing of the ozone recovery for individual scenario depends on other mechanisms, such as changes in the chemical composition of the atmosphere, arising from natural and anthropogenic causes.
- The time for EESC to return to the 1980 level (the EESC recovery date) and the integrated EESC values (to the EESC recovery date) provide useful metrics to compare the relative merits of various emission scenarios.
- There have been suggestions that the mean age of air, and age-dependent release factors should be used in calculation of EESC. This is potentially useful for calculating EESC values that are more representative of polar ozone depletion, in particular. The new recipe will change the absolute values of the metric for global ozone depletion, but should not qualitatively affect the relative benefit estimates of the different scenarios.

Future halocarbon emissions are derived using a new bottom-up approach for estimating emissions from bank sizes. The new method gives future CFC emissions that are higher than previously estimated in WMO (2003).

Updated results on projections of EESC values.

- Current projected concentrations for EESC in the 21st century are higher than reported in WMO (2003) because the most recent CFC bank estimates, which are believed to be more accurate, are larger and lead to larger emissions, and the estimated emissions due to future production of HCFCs from Article 5(1) countries are also larger.
- The EESC in the baseline scenario returns to the 1980 value in the year 2049, about five years later than the date based on the WMO (2003) baseline scenario.
- Compared to the WMO (2007) baseline scenario, cessation of all future emissions will bring the EESC recovery date earlier by 15 years to 2034. Integrated EESC (from 2007 to the EESC recovery date) from ODSs already in the atmosphere as of 2007 is 58% of the integrated EESC for the baseline scenario.
- If no future production is assumed, the date when EESC returns to the 1980 level is moved earlier by six years to 2043. The integrated EESC from ODSs produced after 2007 is 17% of the integrated EESC for the baseline case.
- Results from additional mitigation scenarios (reduction in future HCFC productions and more realistic bank recovery) are also presented.

Direct radiative forcing from ODSs and HFC replacement chemicals is approximately 0.34 W per m^2 in the current atmosphere and is expected to stay below 0.4 W per m^2 through 2100. This is to be compared with forcing from CO_2 of 1.66 W per m^2 in the 2005 atmosphere, increasing to as high as 5 W per m^2 by 2100 for the SRES A1B scenario.

- The bulk of the direct forcing from halocarbons in the current atmosphere is from CFCs (80%), with 10% from HCFCs, 7% from other ODSs, and 3% from HFC.
- Direct forcing from CFCs will decrease to 0.1 W per m^2 by 2100. Direct forcing from HCFCs and other ODSs are expected to be negligible by 2100.
- Forcing from HFCs is 0.15 W per m^2 and 0.24 W per m^2 in 2050 and 2100, respectively, for the SRES A1B scenario while other scenarios indicate that it will be lower. However, current observations suggest that the present atmospheric radiative forcing of the HFCs has been larger than computed for the SRES scenarios, primarily due to higher HFC-23 concentrations.

The (negative) forcing associated with the observed ozone depletion was estimated to be about -0.05 W per m^2 in 1998, corresponding to one-sixth of the direct forcing due to ODSs. If one assumes that all of the observed ozone depletion is due to ODSs, that would imply that the indirect effect is one-sixth of the direct effects for the mix of ODSs present in the atmosphere at that time. Current estimates assume that the indirect forcing from ODSs will decrease to zero when EESC returns to its 1980 levels, while the direct forcing (mainly from CFCs and HFCs remaining in the atmosphere) will continue.

Using available historical and projected United States and global emissions estimates, we find that emissions from the United States contribute between about 15% and 37% to global EESC due to man-made emissions at 2030. For the same year, the United States' contribution to radiative forcing from ODSs, HFCs, and PFCs is 19% to 41%.

5.1 INTRODUCTION

This chapter presents results on how future halogen loading will affect the future behavior of total column ozone and the prospect for the detection/validation of the expected recovery trend. In a hypothetical argument, if the transport circulation, the climate and the background atmosphere were to remain unchanged as of the present-day, the projection of ozone could be based essentially upon future halogen loading. Chapter 2 discussed the concept of equivalent effective stratospheric chlorine (EESC) and how the values for midlatitude EESC and polar EESC could be used to estimate future ozone behavior. Since policy decisions are being made based on EESC, it would be prudent to perform analyses to see how well the EESC-based prediction agrees with model simulations. The reality though is that the atmosphere is changing its composition because of changes in emissions (both natural and human-made), and changes in natural phenomena such as solar cycle and volcanic eruptions. The space-time ozone abundance is also governed by the evolution of climate owing to the effects from changes in stratospheric temperature and transport circulation. Nevertheless, ODSs will remain a driver of human-caused ozone depletion up until 2040 and reductions in emissions of these chemicals represent the only know acceptable method to reduce the associated ozone depletion expected in this period.

The results on numerical simulations of the future behavior of ozone as reported in the WMO (2007, chapter 6) report are presented in section 5.2. The results show that the ozone increase expected between now and 2025 is largely due to the anticipated decrease in halogen loading. The halogen loading is expected to approach its 1980 value towards the middle of the century. In the decades that follow, the effects of climate change and changes in other trace gases will determine the ozone behavior. Section 5.3 discusses how future ozone may affect UV. Sections 5.4 and 5.5 focus on expected future trends of the halocarbons through 2050. The future emissions and abundances of the CFCs and HCFCs are discussed in Section 5.4. The equivalent effective stratospheric chlorine (EESC) will be used to compare the relative impacts of various ODS emission scenarios on future ozone in Section 5.5. Included in this section is a discussion of the radiative forcing associated with the halocarbons as well as the HFCs used as replacements for the ODSs. The contribution from the United States to the future halocarbon loading will be addressed in the context of EESC and radiative forcing in Section 5.6.

5.2 MODEL SIMULATIONS OF THE FUTURE BEHAVIOR OF OZONE

Analyses of the 40+-year time series of global ozone data between 1964 and 2006 (see discussion in Chapter 3, Figure 3.2.1.1-1) indicate that it is possible to attribute the observed ozone behavior to several processes that affect ozone. These include the responses to the seasonal cycle, to the QBO cycle, to the 11-year solar cycle, to episodic volcanic eruptions, and to halogen loading from halocarbons. In particular, the decreasing trend in ozone during this period can be correlated with EESC and attributed to the

increase in halogen loading. It is anticipated that the decrease in halogen loading in the next 20 years will still have a large influence on the decadal trend of ozone. To predict the future trend of ozone, one must identify all processes that may affect ozone, determine how the driving mechanisms may change (*i.e.*, the scenarios), and employ numerical models to simulate the ozone behavior. The projected behavior will depend on the adopted scenario. The results presented in this section show that different models predict different results for the same scenario. This indicates that there is still disagreement on how processes are represented in the models and one must depend on further comparison with observations to resolve these issues. Finally, the purpose for presenting the model results in this chapter is to illustrate, in general terms, how the expected ozone behavior differs from the parameterized behavior based on EESC. It is beyond the scope of this report to address the various outstanding issues associated with simulating ozone behavior. Such attempts would greatly benefit from studies of changes in local ozone as functions of altitude.

5.2.1 Processes and Scenarios Used in Model Simulations

It is clear that the model simulations must include the effects from changes in halogen loadings. The model simulations use prescribed surface concentrations of the halocarbons derived from projected emissions. The method for deriving the surface concentrations from emissions will be discussed in more details in Section 5.4. The current best estimate scenario for future halocarbon surface concentrations (A1) is discussed in the IPCC/TEAP report (2005) and summarized in Table 8-5 of the WMO (2007, Chapter 8) report. Because the chapters in the WMO (2007) reports were prepared in parallel, there

was not sufficient time to use this most updated scenario in the model simulations. The model results presented in Chapter 6 of the WMO (2007) report were simulated using the scenario (Ab) as summarized in Table 4B-2 in the WMO (2003, chapter 4) report.

Using assumed values for the atmospheric lifetimes, the release factors of the halocarbons, and the transport lag from the tropopause, one can compute the date when mid- latitude and polar EESC will reach reaching its 1980 value. This is sometime referred to as the EESC recovery date. For scenarios A1 and Ab, the dates for midlatitude EESC are 2049 and 2045, respectively. However, because of the uncertainties associated with the lifetimes and the release factors, Chapter 6 of the WMO report chose to discuss the results relative to an EESC recovery date between 2040 and 2050. The recovery date for global ozone could be earlier than the EESC recovery date if the net effect from other factors (see below) causes an increase in ozone relative to the 1980 value. Finally, the recovery date for ozone at a specific latitude is likely to be different for different latitudes.

Variations in natural factors such as changes in the Sun's energy output and volcanic events will continue to have impacts on the ozone abundances. Changes in solar UV between cycles are assumed to be small. Effects on ozone from variations within each 11-year cycle can be isolated as demonstrated in Figure 3.2.1.1-1. Once identified, the effect can be removed in interpreting the observed ozone changes. Thus, it is not crucial whether the solar cycle effect is included in the simulations. Effects from volcanoes are not included as there is no reliable way to predict volcanic eruptions in the future. Their

effects can be removed in the analyses several years after it occurs. The philosophy here is that, like the solar cycle, the effect can be removed from the observation before they are compared with the model simulated trends.

Chapter 4 discussed how climate change due to increased CO_2 (and other WMGHGs), change in water vapor in the stratosphere, and changes in long-lived source gases (CH_4 and N_2O) could affect ozone. Climate change can affect ozone through changes in temperature and transport circulation. Cooling of the stratosphere associated with greenhouse gases is expected to slow gas-phase ozone loss reactions and increase ozone. This is particularly effective in the upper stratosphere. As will be discussed in Section 5.5, the forcing from HFCs is small compared to CO_2 and not expected to have a large effect. Water vapor in the stratosphere plays a particularly interesting role. It affects ozone concentration through the hydroxyl chemistry, as well as contributing to the cooling of the stratosphere. Its concentration can be changed due to changes in methane and changes in climate. In the scenario calculations, changes in water are not prescribed. It is calculated from the CH_4 increase and from changes associated with climate in chemistry climate models (CCMs).

The scenario for CO_2, CH_4, and N_2O used in the simulations are summarized in Table 5.1. Based on sensitivity simulations from two-dimensional (2-D) chemistry transport models (CTMs) reported in WMO (1999, chapter 12), a 15% increase in CH_4 at 2050 from its 2000 values would have added about 0.5% in column ozone at midlatitudes. A

15% N_2O increase would have decreased ozone by about 1%. Thus, in the scenario shown, the combine effects from CH_4 and N_2O is to increase ozone around 2050.

The WMO reports also discussed changes in aerosol and NO_x from aviation (WMO 2003, chapter 4); emissions from rocket launches (WMO 2003, chapter 4), and changes in molecular hydrogen (H_2) (WMO, 2007, Chapter 6). Emission of NOx from subsonic airplane increases ozone in the upper troposphere. The IPCC (1999) estimates an increase 0.4% increase in column ozone at midlatitudes in the current atmosphere can be attributed to en route emissions from aircraft. Anticipated doubling to tripling of emission by 2050 could add another 1%. Detailed projection of future emissions based on demands and technology advances are not yet available. Previous estimates suggest that current rocket launch schedule may have caused a small (<1%) column decrease. Future trend will depend on growth and mix of solid fuel and liquid fuel propellants. Estimates for change in H_2 is based on the assumption that liquid hydrogen may become an important energy source for the economy and leakage from storage and usage may cause a dramatic increase in H_2. Not enough is known to do any reliable projection. The effects from these processes are not included in the WMO simulations.

Table 5.1 Future concentrations of CO_2, CH_4, and N_2O used in the model simulations. The CO_2 values are from the ISAM model as listed in Appendix II of IPCC (2001).

	Year										
	2000	**2010**	**2020**	**2030**	**2040**	**2050**	**2060**	**2070**	**2080**	**2090**	**2100**
CO_2 (ppm)	369	391	420	454	491	532	572	611	649	685	717
CH_4 (ppb)	1760	1871	2026	2202	2337	2400	2386	2301	2191	2078	1974
N_2O (ppb)	316	324	331	338	344	350	356	360	365	368	372

5.2.2 Results from Model Simulations

Three types of models were used to simulate the future behavior of ozone in WMO (2007, Chapter 6):

1) Two-dimensional chemistry-transport models (2-D CTMs) use fixed temperature and circulation. They are most useful for isolating the effects of different source gases;
2) Interactive 2-D models partially account for the changes in circulations associated with climate change by calculating the residual circulation from heating rates. However, the feedback from changes in wave forcing is not simulated; and
3) Three-dimensional climate chemistry model (3-D CCMs) incorporate all the identified feedbacks and are generally better able to represent the key processes related to 3D transport in the atmosphere (particularly the polar regions).

In the following discussion, both the observation and the model results will be displayed as annual mean or monthly anomalies expressed as a percentage of the pre-1980 conditions. The midlatitude EESC recovery date is expected to occur sometime between 2040 and 2050. Much attention was paid to comparing the ozone recovery date (the date when the simulated ozone anomaly returns to its 1980 value) to the EESC recovery date. It has proved convenient to examine the spatial aspects of the problem in terms of the phenomena in the two polar regions (Arctic and Antarctic) and that in the tropics plus midlatitudes (~60N-S). This separation accounts for the distinct stratospheric circulation patterns prevailing in the climate system, is relevant for compartmentalizing approximately the ozone chemical-dynamical interactions, and represents a convenient way to look at the “big” global picture.

6350

6351 **5.2.2.1 Tropics and midlatitudes**

6352 Figure 5.1 shows the simulated future behavior of column ozone from interactive 2-D
6353 models (solid lines) and non-interactive 2-D CTMs (dashed lines). The models' hind-cast
6354 predictions are compared with observations as a way to screen the 2-D CTMs. All 2-D
6355 models show that ozone amount increases with time between 2007 and 2050. The model
6356 spread among the non-interactive 2-D CTMs for northern midlatitudes is about 3% at
6357 2050. The WMO (2007, Chapter 6) report did not discuss how changes in N_2O and CH_4
6358 contributed to the individual model results. Based on the estimates given above and the
6359 scenario stated in Table 5.1, it would appear that CH_4 is adding about 1% while the effect
6360 of N_2O is to decrease ozone by about 0.5% in 2050. It is also evident from the figure that
6361 the sensitivities in these models differ.

6362

6363 Results from the interactive 2-D models show that the ozone anomaly is larger by about
6364 2% in 2050 and 4% in 2100. The effect at midlatitudes is larger at about 3% in 2050. This
6365 is consistent with the expected ozone increase due to cooling in the stratosphere. There is
6366 no clear indication on the effect of increased upwelling in the tropics though this could
6367 have been masked by the ozone increase in the upper stratosphere due to the cooling.

6368

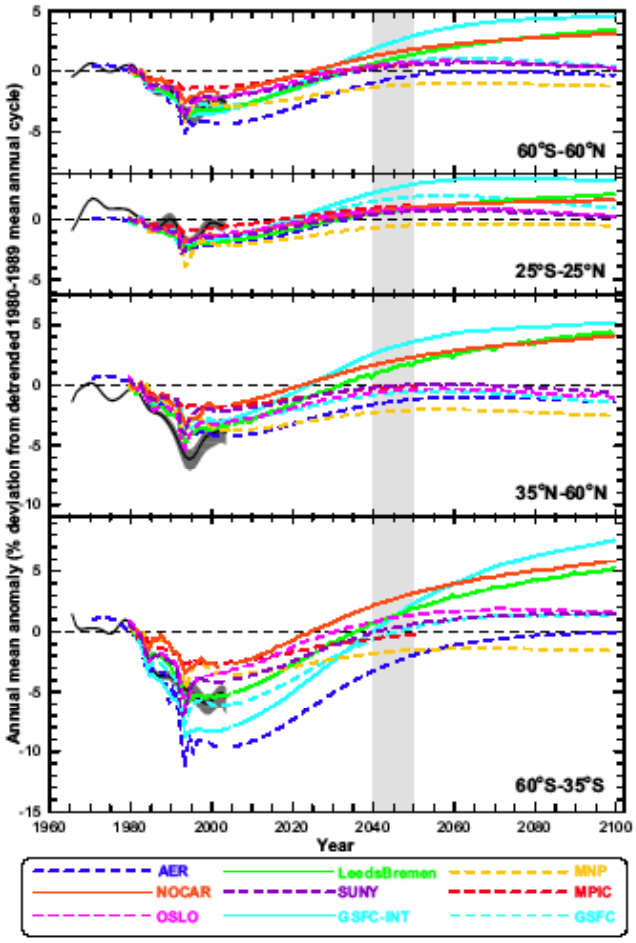

Figure 5.1 Simulated annual mean ozone anomaly from 2-D models for different latitude bands. Results from interactive models are designated by solid lines. The figure is identical to Figure 6-9 in WMO (2007). See Eyring *et al.* (2006) for details on how the annual mean anomaly is computed. The black line with the grey shade represents the observed mean values and the range. The grey vertical band marks the time period when midlatitude EESC is expected to recover to the 1980 value.

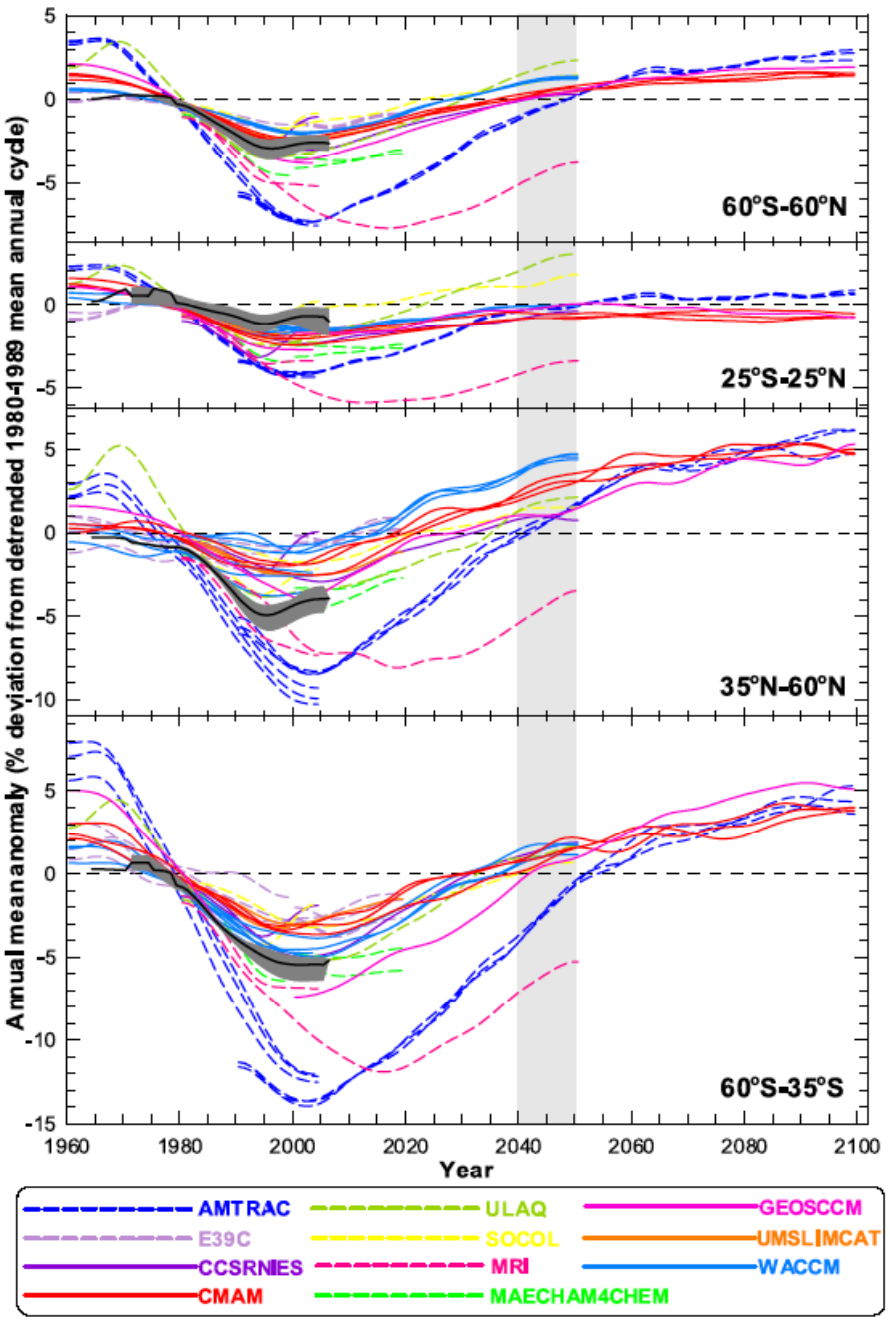

Figure 5.2 Results from 3-D CCMs. The figure is the same as Figure 5 in Eyring *et al.* (2007) which includes additional model results computed after publication of the WMO (2007) report. See Eyring *et al.* (2006) for details on how the annual mean anomaly is computed. The solid line with the grey shade represents the observations with uncertainty. The grey vertical band marks the time period when midlatitude EESC is expected to recover to the 1980 value

Results from 3-D CCMs are shown in Figure 5.2. Several tests were used to identify models that successfully simulate parameters important for ozone response to halogen

loading (see Eyring *et al.*, 2006). Models that perform better in those tests are identified using solid lines in Figure 5.2. For our purpose, we concentrate on the three models (CCSRNIES, CMAM, and WACCM) that "earned" the solid line rating and performed the REF2 simulations from 1980 to 2050. Other models performed the REF2 simulation starting in 1990 or 2000 making it difficult to compare the ozone anomaly at 2050 to the anomaly at 1980 to determine the ozone recovery date. For ozone content between 60S and 60N, the recovery dates are 2030 for WACCM, 2040 for CMAM and CCSRNIES. All three models show little ozone increase beyond the 1980 values in the tropics, consistent with the expectation that increase in upwelling is suppressing ozone. This is evident in the model-simulated decrease in tropical ozone below 20 mb (see Figure 6(b) in Eyring *et al.*, 2007). The ozone recovery dates for northern midlatitudes are 2010 for WACCM, 2020 for CMAM, and 2030 for CCSRNIES. The recovery dates for the southern midlatitudes are all between 2030 and 2040. The CMAM model presented results through 2100. The ozone anomaly in the northern midlatitude is around 5%, well beyond the calculated anomaly for 1960 (~0.5%).

To isolate the effects of climate change, three CCMs performed a simulation where the surface concentrations of the GHGs were kept fixed at their 1970 value (Figure 5-25 in Chapter 5, WMO 2007). The results from WACCM show that in the absence of these GHG forcing, the ozone recovery date for 60S – 60N is around 2040 and the ozone amount in 2050 is about 1% smaller. Unfortunately, the run also kept the surface concentrations of CH_4 and N_2O fixed. Thus, the 1% effect results from both climate change and the direct chemical effects of CH_4 and N_2O.

6409

6410 **5.2.2.2 Polar region**

6411 Figure 5.3 shows the model simulated ozone anomalies for the Arctic and the Antarctic
6412 regions. Most models show larger anomalies in the Antarctic, consistent with the fact that
6413 the temperature is colder leading to formation of more PSCs, and the vortex are more
6414 confining. Within almost all models, the Arctic ozone recovery date is much earlier than
6415 the Antarctic ozone recovery date.

6416

6417 The polar EESC recovery date is estimated to be between 2060 and 2070. We will again
6418 concentrate on the results from CCSRNIES, CMCM, and WACCM for the reason
6419 discussed in the previous section. The Arctic polar ozone recovery dates are 2000 for
6420 CCSRNIES, 2010 for CMCM, and 2015 for WACCM. Once the ozone anomaly reaches
6421 the 1980 value, it increases smoothly to beyond the 1960 anomaly.

6422

6423 The exact time evolution of the Antarctic ozone hole is different depending on the
6424 diagnostics chosen. These include ozone amount in October, minimum ozone in
6425 September and October, ozone mass deficit, and maximum Antarctic ozone hole area
6426 between September and October. The minimum ozone value is projected not to increase
6427 until after 2010 in several models, while decrease in ozone mass deficit in most models
6428 has occurred by 2005. If we use the ozone content pole ward of 60 calculated by the three
6429 models as the metric, the ozone recovery dates are up to 30 years earlier. The CMAM and
6430 WACCM models produced ensemble results. The three simulations from the WACCM
6431 model produced polar ozone recovery dates between 2030 and 2040, while those from

6432 CMAM are between 2040 and 2060. The CMAM results also showed that the value for
6433 the Antarctic ozone anomaly stays closed to zero for about 20 years after the initial
6434 recovery before taking off.
6435

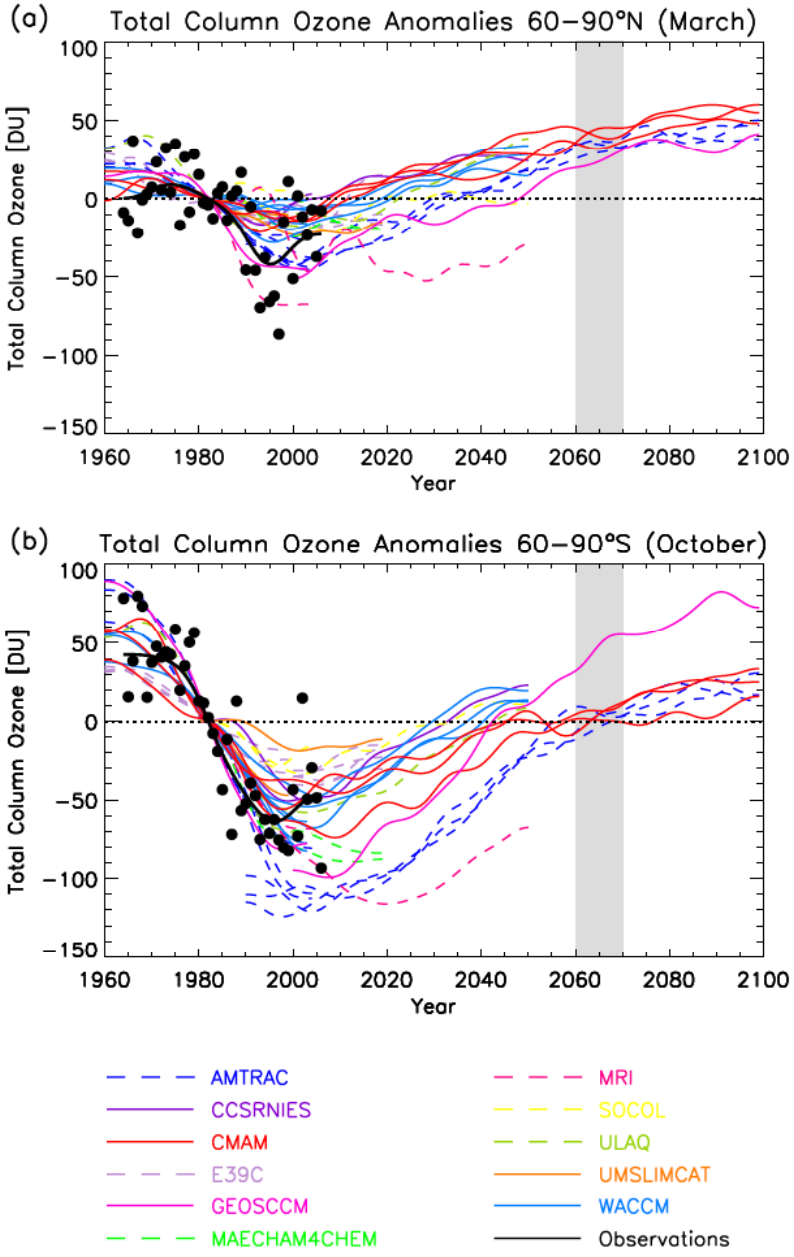

6436
6437 **Figure 5.3** Zonal mean monthly ozone anomalies for Artic in March (upper panel) and Antarctic in
6438 October (lower panel). The figure is identical to Figure 7 in Eyring *et al.* (2007) updated to include
6439 additional results after the publication of WMO (2007) report. The observations are shown as black dots
6440 and a smooth curve representing the mean value. The grey vertical band marks the time period when polar
6441 EESC is expected to recover to the 1980 value.

5.2.3 Stages of Ozone Recovery from ODSs

A good portion of Chapter 6 in the WMO (2007) report was devoted to discussion of the detection and attribution of the expected ozone recovery. For detection of changes in trend that already occurred, one must deduce a statistically significant change in trend above the variability. The expectation is that it would be easier to detect such changes outside of the polar regions where the year-to-year variations are expected to be smaller. In the context of this report, the attribution issue is whether EESC is a good proxy for future ozone behavior so that one could have confidence that policy decisions based on EESC would achieve the goal of ozone recovery. Indeed, there are concerns (*e.g.*, Hadjinicolaou *et al.*, 2005) that improper interpretation of the recent observed ozone increase after the late 1990s may give the wrong impression that the effects of halogen on ozone has been overestimated and one should relax the reduction strategy.

In the absence of other changes, it is expected that ozone will stop decreasing around the time when EESC peaks (around 1997). As EESC decreases, ozone will increase to its 1980 value around the time EESC recover to its 1980 value around 2050 (see Figure 6-1 and associated discussion in Chapter 6 of the WMO (2007) report). Note that even in the absence of other changes, the timing between EESC recovery and ozone recovery is uncertain for the following reasons. First, there is uncertainty in the EESC recovery date from uncertainties in the assumed lifetimes and release factors. Comparison between EESC recovery date and model-predicted ozone recovery date is complicated by the fact that the lifetimes and release factors in the model are likely to be different from what is

assumed in the EESC calculation. To resolve this issue, comparison and validation of model-simulated atmospheric lifetimes and release factors should be a priority. Once this is done, one can then perform simulations using emissions and compare the timing between ozone recovery and EESC recovery as calculated by the model.

The work of Yang *et al.* (2006) clearly shows that the length of observations required to detect such change depends on the quality of the data. Given the current results, it is anticipated that we should be able to confirm whether ozone is increasing due to decrease in halogen loading in the next five or six years. We are not in a position to predict precisely when ozone recovery will occur and recognize it as such as soon as it occurs. Nonetheless, the simulations give confidence that one should be able to confirm the ozone recovery after the fact by waiting several years to analyze the observations and removing the interannual variability.

Chapter 6 identified other factors that could complicate the attribution of the observed changes. These include changes in atmospheric compositions other than the halogens, changes in temperature and transport circulation, changes in solar cycle and volcanic eruptions. The largest effect on short-term (five to ten years) trend is expected to come from changes in transport circulation. The study of Yang *et al.* (2006) concluded that half of the observed increase in ozone between the late 1990s and 2005 could be attributed to changes in transport circulation in the lower stratosphere. This is not unexpected since while EESC has stopped increasing, it essentially remained unchanged during this period Hadjinicolaou *et al.* (2005) had a similar conclusion using a very different approach. The

6488 authors use a 3-D CTM to calculate the ozone from 1979 to 2003. The CTM uses the
6489 transport circulation from the ERA-40 ECMWF analyses. The ozone chemistry is
6490 parameterized with the local loss frequency fixed at the 1980 conditions. The conclusion
6491 is that the ozone trends between 1994 and 2003 derived from the modeled and observed
6492 ozone agree indicating that change in transport is the main driver in this time period. The
6493 paper also concluded that the model calculated ozone showed a decreasing trend
6494 between1979 and 1993, and the trend is around one-third of the trend derived from
6495 observation. More analyses (such as additional model results using full chemistry to show
6496 that the derived trend is not significantly larger than the observed trend) are needed to
6497 support this last conclusion that changes in transport are responsible for one-third of the
6498 observed ozone trend between 1979 and 1993.
6499
6500 Other changes are more important after 2050 when effects from other changes (changes
6501 in CH_4, N_2O and CO_2) will dominate. If the desire is to understand future ozone behavior
6502 beyond the effects of halogens, one should pay more attention to the trends of the other
6503 source gases and try to determine to what extent one could separate the effects in the
6504 future observations.
6505
6506 **5.3 EXPECTED RESPONSE IN SURFACE UV**
6507 Ozone column in the atmosphere is one of many factors that affect UV at the ground. The
6508 UV community recognizes the importance of variations in aerosol, clouds, and surface
6509 albedo on UV. The effect of ozone change on cloud through climate feedback has not
6510 been quantified at this point, but is expected to be small.

If everything else is assumed to be constant, the future UV trend will depend on the anticipated ozone change. Within the limitation that applies to EESC as a proxy for future ozone behavior, it can likewise be used as a predictor for UV. However, most UV predictions are done locally at specific latitudes, thus the relationship between EESC and typical midlatitude ozone depletion is not particularly useful. In practice, model simulated ozone changes at specific latitudes are fed into a radiative transfer model to compute the change in UV irradiance. An example of such a calculation is shown in Figure 5.4, which shows the calculated noon-time erythemal irradiance at several latitudes. Note that the recovery at southern polar latitude occurs much later than the midlatitude values, reflecting similar behavior of midlatitude and polar ozone columns as indicated in the results from the AMTRAC model in Figure 5.2.

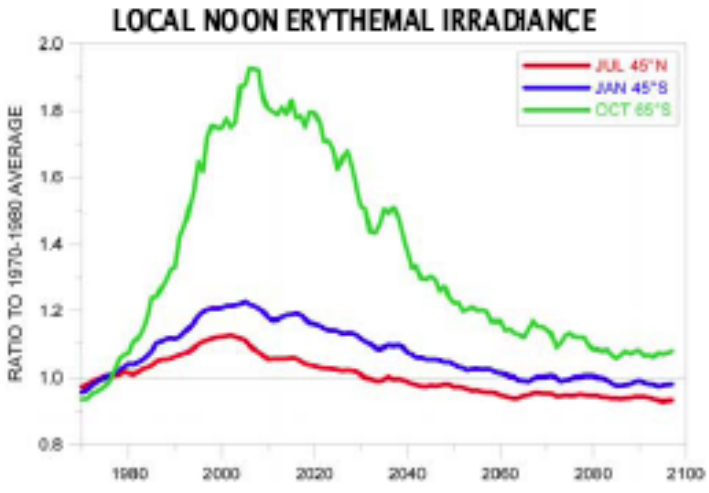

Figure 5.4 Estimated changes in erythemally weighted surface UV irradiance at local noon in response to projected changes in total column ozone as calculated by the AMTRAC CCM (see blue dashed curve in Figure 5.2) for the period 1970 to 2099, using zonal-averages in total ozone in the latitude bands 35°N-60°N, 35°S-60°S, and 60°S-90°S, and the solar zenith angle corresponding to 45°N in July, 45°S in January, and 65°S in October, respectively. At each latitude, the irradiance is expressed as the ratio to the 1970 to 1980 average. The results have been smoothed with a five-year running mean filter to remove some of the year-to-year variability in the ozone predictions in the model.

5.4 FUTURE SCENARIOS FOR ODSs AND THEIR REPLACEMENTS

We adopt the same "baseline" emissions (A1) scenario that was presented in WMO (2007) which considers only relatively long-lived (lifetime > 0.5 years) chlorine and bromine source gases. However, it has become clearer that very short-lived (VSL) ODSs also contribute to stratospheric ozone depletion. A more detailed discussion of the contribution of VSL compounds to stratospheric chorine and bromine loading can be found in Chapter 2 of WMO (2007). Note that the standard procedure for estimating EESC from emissions of long-lived source gases (as described in Box 2.6 in Chapter 2) should not be applied to VSL source gases. It was estimated in WMO (2007) that VSL compounds might contribute 50 ppt of stratospheric chlorine and 3-8 ppt of stratospheric bromine. It was unclear whether any trend in these VSL compounds should be expected in the future or has occurred in the recent past. Enhancement in convective activities associated with future climate changes may increase the ozone depletion potentials of the VSL species.

5.4.1 Baseline Scenario

In general, the historical portion of the baseline (A1) scenario is based on the observed mixing ratio time series, while future emissions are estimated using the most current information regarding expected future demand of ODSs, future banks, and current

constraints placed by the Montreal Protocol. While this scenario consists of reasonable assumptions about the future, it does not represent a prediction and future levels could be higher or lower depending on, for example, future policy actions and consumer choices. However, it represents a useful projection that is used to examine the sensitivity of ODS abundances to choices concerning future production, banks, and emission.

The mixing ratios used to calculate the historical emissions are obtained primarily from atmospheric observations made by the Earth System Research Laboratory/Global Monitoring Division (ESRL/GMD) (formerly Climate Monitoring and Diagnostics Laboratory, CMDL), the Advanced Global Atmospheric Gases Experiment (AGAGE), and the University of East Anglia (for halon-1211). South Pole firn observations are also considered for CH_3Cl and CH_3Br emissions before 1996. A box model is used to determine the emissions of the species for each year through 2005 using the observed mixing ratio time-series and its current best estimate of the steady state global atmospheric lifetime. Hence, when the same box model and lifetimes are used to calculate the surface mixing ratios from the derived emissions, they produce mixing ratios in the baseline scenario that are exactly equal to the observationally-based time series given in Table 8-5 of WMO (2007). The same box model and lifetimes are used to derive the mixing ratio of each species after 2005 based on projected emissions.

Projections of future demand and sizes of banks are taken from IPCC/TEAP (2005). This information is used along with best estimates of future production to estimate future emissions. Details of these calculations can be found in WMO (2007). The use of future

demand and bank sizes from IPCC (2005) in WMO (2007) represents an important departure from the approach used in previous WMO reports. Previously, the evolution of the estimated bank sizes were calculated solely using the difference between estimated annual production and emission. This approach had the potential to lead to accumulating large errors in the bank sizes because the bank often represents a difference between the two relatively large production and emission values. The IPCC (2005) demand and bank estimates, however, are based on inventories of equipment, an approach often referred to as a "bottom-up" method. Hence, these estimates are independent of systematic errors in production or emission. It is believed that this new approach has led to better future emissions projections.

Comparisons between future emissions projections of WMO (2003) and WMO (2007) demonstrate that the most substantial differences arise for CFC-11, CFC-12, CCl_4, and the HCFCs. The increase in the CFC emissions in WMO (2007) is primarily due to larger bank estimates of the bottom-up approach than were estimated by WMO (2003). The greatest HCFC emission difference is for HCFC-22 and is due to the substantially larger estimated future consumption of this compound by Article 5(1) countries. CCl_4 emissions are currently estimated to be higher than those of WMO (2003) based on observed mixing ratios consistent with a smaller decrease in emission over the last few years and the continued inability to account for all CCl_4 emissions. The resulting differences in mixing ratios are discussed in section 5.4.3.

5.4.2 Alternate Scenarios

Alternative scenarios and test cases were examined in WMO (2007) to examine the relative effects of making various production and/or direct emission reductions on EESC. Three cases for different ODS groups are designed to address three issues: (1) no future emission; (2) no future production; and (3) no future release from the 2007 bank. Results from the "no future emission" case provide the loadings due to the decay of the ODSs already in the atmosphere. It represents the greatest theoretically possible reduction in the future atmospheric burden of the particular compound (short of processing the air to remove the ODSs). The "no future production" case quantifies the importance of new production relative to future emissions, while the "no future release from the bank" quantifies the benefit of the one-time sequestration and destruction of 2007 global bank from future emissions. Additional cases are presented here that examine the effect of recovering and destroying the total estimated United States bank and the United States accessible bank in 2009. Estimates of these bank sizes and the technique used by the U.S. EPA to calculate these estimates are discussed in chapter 2.

WMO (2007) also examined three alternative cases involving CH_3Br. Two cases involved removing quarantine and pre-shipment uses from 2015 onward and continuing critical use exemptions at 2006 levels into the future. The third case explored the importance of the assumption that the 1992 anthropogenic emission represented 30% of the total. Recent mixing ratio observations have suggested that this might be an overestimate with a more accurate percentage falling somewhere between 20% and 30%. These results are discussed in Table 5.2.

A scenario based on the mitigation scenario described in IPCC (2005) is also examined to quantify the effect of this carefully considered set of future policy options. The mitigation scenario only has a substantial effect on the bank of HCFC-22 in the scenario considered here.

After the WMO (2007) report and IPCC (2007) reports were written, the parties to the Montreal Protocol voted to strengthen the HCFC regulations on both Article 5 and non-Article 5 countries. Approximations for the effect of this strengthening are discussed in Section 5.5.1.1.

5.4.3 Time Series of Source Gases

The mixing ratios of the current baseline scenario are compared with those of the WMO (2003) baseline scenario, and the "no future production" and "no future emission" test cases in Figure 5.5. The differences between the WMO (2007) and WMO (2003) baseline scenarios are apparent for several gases, with the differences for HCFC-22 particularly apparent. More modest, but also important are the differences for CFC-11 and CFC-12. The HCFC-22 difference is due to the increase in the expected future consumption of Article 5(1) countries of the Montreal Protocol, while the increase in the CFCs is due to the larger bank size estimates of IPCC (2005). HCFC-141b, HCFC-142b, and halon 1301 show reduced mixing ratios in the short term compared to WMO (2003) owing to the reduced observed growth rates between 2001 and 2004 and the expectation of lower future emissions.

The importance of future projected production and bank sizes to future emission is also apparent for the various compounds. For example, the "no future production" curve for CFC-12 is only slight different from the baseline curve; hence the bank of CFC-12 is expected to dominate future emission, with its effect represented by the difference between the "no future emission" and "no future production curves". The relative importance of future production compared to the amount in the banks varies strongly among the ODSs, with the future abundances of CFC-11 depending primarily on its bank and HCFC-22 future abundances depending primarily on future production. No bank is considered in the future projections of CCl_4, CH_3CCl_3, and CH_3Br.

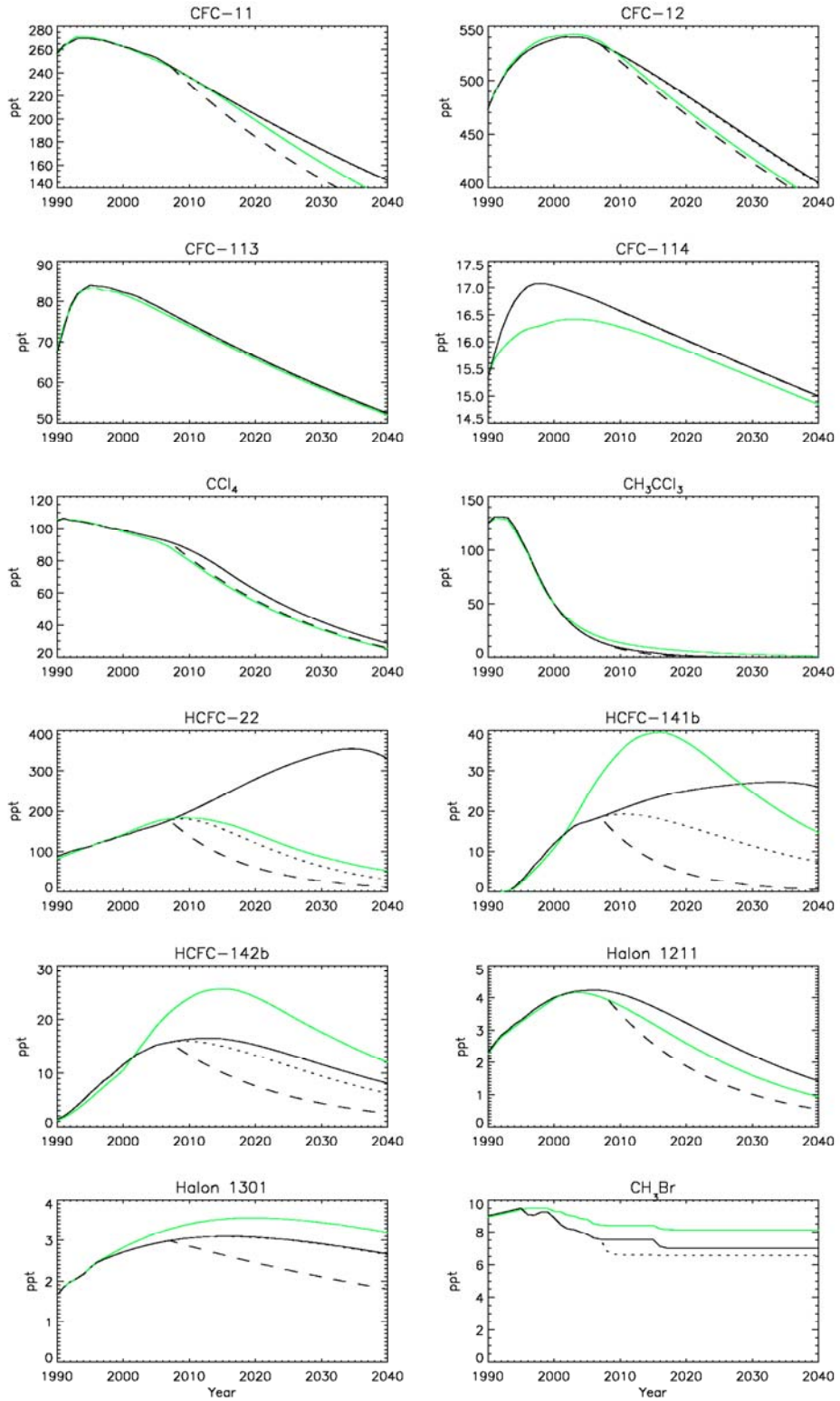

Figure 5.5 Mixing ratio comparisons of WMO (2007) baseline scenario (solid black) with the baseline scenario from WMO (2003) (green), the "no future emission" test case (dashed) and the "no future production" case (dotted curve). Note that different vertical scales are adopted for sub panels and some of the plotted values do not start from zero. For several of the gases, the solid black curve obscures the dotted or dashed curves.

5.5 CHANGES IN INTEGRATED EESC AND RADIATIVE FORCING

5.5.1 Time Series of EESC

5.5.1.1 Midlatitudes

The evolution of ODS mixing ratios cannot, by themselves, be used to accurately quantify the ozone destruction due to those ODSs. The established relationship between stratospheric ozone depletion and inorganic chlorine and bromine abundances suggest that the temporal evolution of inorganic chlorine- and bromine- species in the midlatitude lower stratosphere is an important indicator of the potential damage of anthropogenic activity on the health of stratospheric ozone. Equivalent effective stratospheric chlorine (EESC) was developed to relate this halogen evolution to tropospheric source gases in a simple manner (Daniel *et al.*, 1995; see also Box 2.6 in Chapter 2). This quantity sums ODSs, accounting for a transit time to the stratosphere, for the greater potency of stratospheric bromine (Br) compared to chlorine (Cl) in its ozone destructiveness with a constant factor (α), and also includes the varying rates with which Cl and Br will be released in the stratosphere from different source gases. EESC has been used to relate predictions of human-produced ODS abundances to future ozone depletion (WMO, 1995, 1999, 2003, 2007). The values for midlatitude EESC discussed here are calculated for WMO (2007) using a constant lag time of three years from the ODS mixing ratios and release factors given in WMO (2007). Recent development on how to apply EESC to polar ozone and refinements in using the mean age of air will be discussed in Sections 5.5.1.2 and 5.5.2 respectively.

The relative contribution of various ODSs and ODS groups to midlatitude EESC are shown as a function of time from 2000 to 2100 on the left-hand side of Figure 5.6. The prominent role of CFCs today and into the future is apparent. The slow decline of the contribution from CFCs is primarily due to the relatively long atmospheric lifetimes of the species in this group of compounds and what is already in the atmosphere, and not to continued emission, although continued emission does play a small role. The importance of the halons and CH_3Br, all bromine-containing source gases, is also clear even though their atmospheric concentrations are substantially smaller than those of the dominant chlorine-containing ODSs. This is caused by stratospheric bromine being much more effective than chlorine for stratospheric ozone destruction. As stated in Chapter 2, WMO (2007) has estimated that a molecule of bromine is 60 times more important than a molecule of chlorine for global stratospheric ozone destruction. The lower panels show the change in EESC due to the elimination of production and emission for CFCs, HCFCs, halons, and CH_3Br.

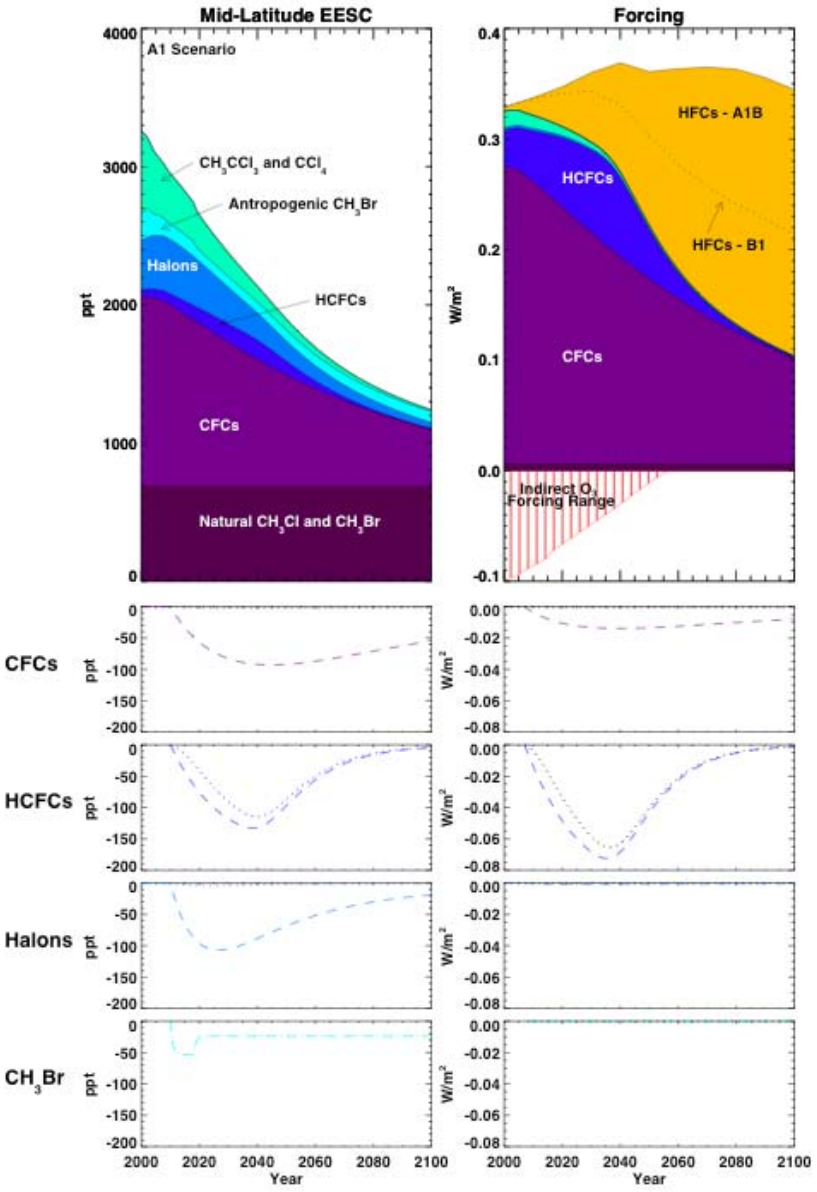

Figure 5.6 EESC and direct radiative forcing estimates from 2000 to 2100 for the baseline scenario (upper panels), and expected decreases relative to the baseline scenario due to a cessation of emission (dashed curves) and production (dotted curves) in 2007 for CFCs, HCFCs, halons, and anthropogenic CH_3Br. The left half of the figure is from Figure 8-5 in WMO (2007). Note the difference in the vertical scales between the top panel and the bottom four panels. The "no production" curve for CFCs and Halons lies almost on the zero line, indicating that future productions of these ODSs play a very small role in the baseline scenario. In contrast, the contribution from the HCFCs is mostly due to future productions. The "no emission" and "no production" curves are identical for CH_3Br because no bank was considered in its projections. The HFC forcing is shown for the B1 and A1B SRES scenarios. The indirect forcing due to ozone depletion caused by ODSs is included for comparison, but should be considered only a rough approximation.

In the past, EESC estimates have been used to evaluate various ODS emission scenarios primarily using two metrics. They are: (1) a comparison of the times when EESC returns to 1980 levels, the so called EESC recovery date; and (2) the relative integrated changes in EESC between 1980 and the corresponding EESC recovery date. Figure 5.7 demonstrates that the time for midlatitude EESC to return to the 1980 level is currently expected to occur around 2049 for the baseline scenario, five years later than projected in WMO (2003). This later return was primarily ascribed to higher estimated future emissions of CFC-11, CFC-12, and HCFC-22. The increase in CFC emissions is due to larger estimated current bank sizes, while the increase in HCFC-22 emissions is due to larger estimated future production. The soonest that a complete theoretical elimination of emission could lead to an earlier return is 2034. Elimination of all future ODS production is expected to lead to a return to 1980 EESC levels in 2043, while an elimination of the 2007 bank is expected to lead to a return in 2041.

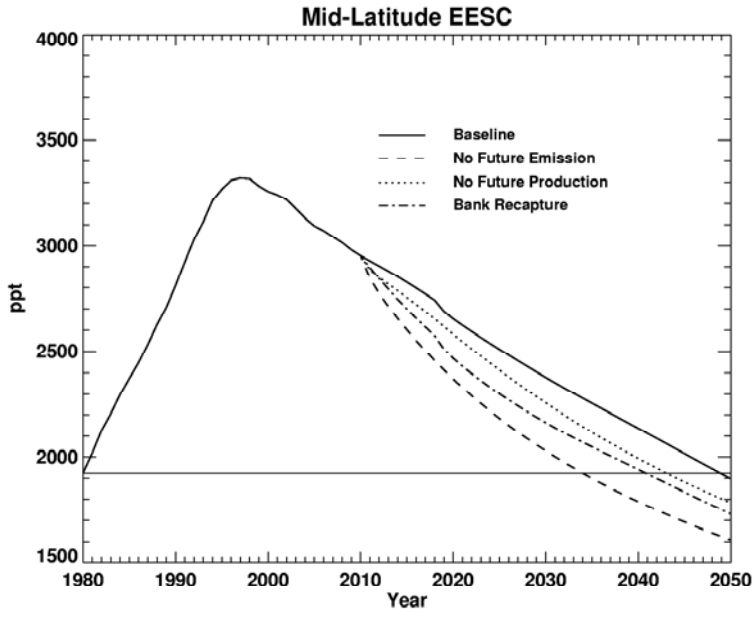

Figure 5.7 EESC estimates from 1980 through 2050 for the baseline scenario, the three comparative test cases considered in WMO (2007). The horizontal line represents the 1980 EESC level.

A detailed partitioning of the effects of reductions in the various ODS groups is shown in Table 5.2. The years when EESC is expected to return to 1980 levels are also included in the table for midlatitudes. The Antarctic ozone response to EESC will be discussed in more detail in section 5.5.1.2. The table illustrates that the elimination of the future emissions of CFCs, HCFCs, and halons represents the greatest potential for reducing future ozone depletion. To accomplish this elimination for CFCs and halons, banks would have to be captured and destroyed because future emission is expected to be dominated by the release from banks. For HCFCs, future production plays a larger role in future emission than do the current banks, so emission from both banks and future production would have to be eliminated. The technical difficulty and expense involved with capturing banks depends on the nature of the banks, while the feasibility of reducing future production will depend on replacement options for the pertinent applications. More details concerning the nature of the various ODS uses and bank types and the options available for reducing future ODS emissions can be found in other reports, including IPCC (2005) and UNEP/TEAP (2007). It should also be recognized that these full bank recovery and zero production and emission test cases shown in Table 5.2 are meant as hypothetical cases against which more realistic scenarios can be compared. This procedure is used in Section 5.6 to evaluate the significance of the United States ODS banks.

The results for the scenario representing the IPCC (2005) mitigation scenario are not shown in Table 5.2, but this scenario leads to an EESC response that is approximately

6752 20% of the zero-emission case for the HCFCs, due primary to actions to reduce the
6753 HCFC-22 bank emission.
6754
6755 Future emissions of CH_3Br also have the potential to be as important as each of these
6756 three classes of compounds. The continuation of the critical use exemption at the 2006
6757 level and the continuation of QPS uses both have a substantial impact on global EESC.
6758
6759 In late 2007, the Montreal Protocol HCFC restrictions for both production and
6760 consumption were strengthened, partly in response to the renewed awareness of the
6761 importance of HCFCs to climate forcing in addition to ozone depletion. While
6762 restrictions were tightened for both Article 5 and non-Article 5 countries, the changes for
6763 the Article 5 countries are much more significant for stratospheric ozone. In Figure 5.8,
6764 the former Protocol HCFC restrictions for Article 5 countries are compared to the newly
6765 passed ones, as well as to the United States proposal that contributed to the strengthened
6766 restrictions. An additional curve is also shown that represents the closest scenario
6767 calculated in UNEP/TEAP (2007). For the TEAP scenario, it is estimated that integrated
6768 EESC is reduced by 2.6% and 5.6%, respectively, for the integration from 1980 to the
6769 return of EESC to 1980 levels and from 2007 to the return to 1980 levels. This is a
6770 substantial reduction even when compared to the zero emissions case for HCFCs in Table
6771 5.2. The baseline HCFC emissions are slightly higher in UNEP/TEAP (2007) than those
6772 assumed in WMO (2007), making the effect of HCFC reductions correspondingly
6773 slightly higher. This TEAP report also examines other “practical options” that could be
6774 usefully employed to reduce future emissions of HCFCs and other ODSs. These include

6775 emission reduction measures during the use phase of applications and equipment, from
6776 design and material section alternatives, from end-of-life management, and due to early
6777 retirement of equipment. These measures were submitted by the Parties to the Montreal
6778 Protocol and organized at the 26th Open-ended Working Group of the Parties to the
6779 Montreal Protocol. The TEAP report finds that a combination of earlier HCFC phase out
6780 described above with these additional "practical measures" leads to an integrated EESC
6781 reduction of 7.4% and 16.0% percent, respectively, for the integration from 1980 to the
6782 return of EESC to 1980 levels and from 2007 to the return to 1980 levels.
6783

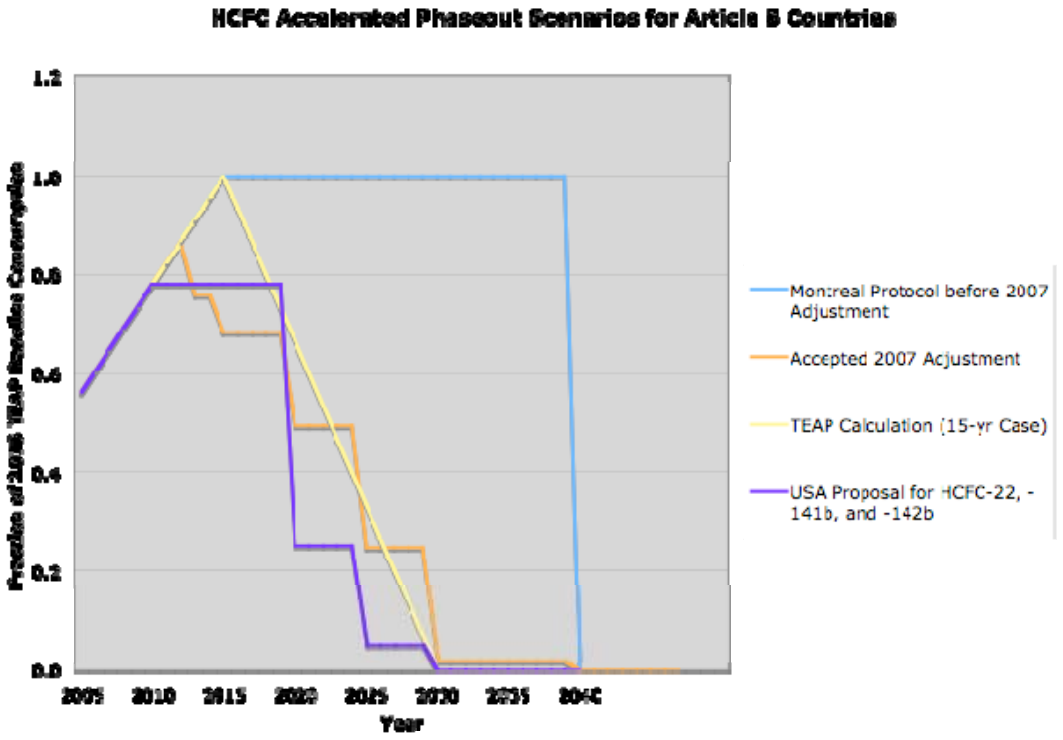

6784
6785 **Figure 5.8** Comparison of alternate scenarios for future emissions of HCFCs.
6786

6787 **5.5.1.2 Polar regions**

Compared to midlatitude EESC, Arctic EESC is less useful as a proxy for polar ozone depletion because interannual variability in meteorology has a much larger impact on the ozone response to inorganic halogen loading. In the core of the Antarctic vortex during early spring, the interannual variability is small, suggesting that EESC provides a useful proxy for ozone hole recovery (Newman *et al.*, 2006). The far right column in Table 5.2 shows the results calculated using a time lag of six years and the same release factors based on midlatitude measurements. Because of the larger time-lag, the polar EESC value in 1980 is smaller than the 1980 midlatitude value. In addition, the larger lag time also makes the polar EESC value larger than the midlatitude EESC value in 2050. Therefore, the polar EESC recovery date is 15 to 17 years later than the midlatitude EESC recovery date.

Table 5.2 Comparison of scenarios and cases[a]: the year when EESC drops below the 1980 value for both midlatitude and polar vortex cases, and integrated EESC differences (midlatitude case) relative to the baseline (A1) scenario.

Scenario	Percent Difference in integrated EESC relative to baseline scenario for the midlatitude case		Year (x) when EESC is expected to drop below 1980 value	
	Midlatitude			Antarctic vortex[b]
	$\int_{1980}^{x} EESC\,dt$	$\int_{2007}^{x} EESC\,dt$		
Scenarios				
A1: Baseline scenario			2049	2065
Cases[a] of zero production from 2007 onwards of:				
All ODSs	-8.0	-17.1	2043	2060
CFCs only	-0.1	-0.3	2049	2065
Halons only	-0.2	-0.5	2049	2065
HCFCs only	-5.5	-11.8	2044	2062
Anthropogenic CH_3Br only	-2.4	-5.1	2048	2063
Cases[a] of zero emissions from 2007 onwards of:				
All ODSs	-19.4	-41.7	2034	2050
CFCs only	-5.3	-11.5	2045	2060
CH_3CCl_3 only	-0.1	-0.2	2049	2065
Halons only	-6.7	-14.4	2046	2062
HCFCs only	-7.3	-15.7	2044	2062

CCl_4 only	-1.3	-2.9	2049	2065
Anthropogenic CH_3Br only	-2.4	-5.1	2048	2064
Cases[a] of full recovery of the 2007 banks of:				
All ODS	-12.9	-27.8	2041	2057
CFCs only	-5.2	-11.3	2045	2060
Halons only	-6.7	-14.3	2046	2062
HCFCs only	-1.9	-4.1	2048	2065
CH_3Br sensitivity:				
Same as A1, but CH_3Br anthropogenic emissions set to 20% in 1992[c]	3.1	6.6	2051	2068
Same as A1, but zero QPS production from 2015 onwards	-1.5	-3.2	2048	2064
Same as A1, but critical use exemptions continued at 2006 level	1.9 -2.2	4.0–4.7	2050	2067

a) Importance of ozone-depleting substances for future EESC were calculated in the hypothetical "cases" by setting production or emission of all or individual ODS groups to zero in 2007 and subsequent years or the bank of all ODS or individual ODS groups to zero in the year 2007 alone. These cases are not mutually exclusive and separate effects of elimination of production, emissions and banks are not additive.
b) Calculated using a lag time of six years and the same release factors as in midlatitudes.
c) In the baseline scenario this fraction was assumed to be 30% in 1992 with a corresponding emission fraction of 0.88 of production. In this alternative scenario an anthropogenic fraction was assumed to be 20% with an emission fraction of 0.56 of production. In both scenarios the total historic emission was derived from atmospheric observations and a lifetime of 0.7 years.

5.5.2 EESC and Mean Age of Air

Previous EESC calculations have not included a distribution of transport times from the troposphere into the stratosphere (the so called age-of-air spectrum) or any dependence of the fractional chlorine release value on the age-of-air. Newman *et al.* (2006) reformulated EESC to account for both an age-of-air spectrum and age dependent fractional release rates. Those results were discussed in Box 8-1 of WMO (2007). In this section, we will summarize how the EESC estimates derived from Newman *et al.* (2006) differ from the results in Section 5.5.1.2.

The dashed lines show EESC for mean ages of 3.0 y (blue) and 6 y (red) as estimated using the Newman *et al.* (2006) technique, while the solid lines show EESC for constant

6825 age shifts (time-lags) of 3.0 y (blue) and 6 y (red). The solid lines duplicate the EESC
6826 used in WMO (2007). The main difference in the recovery dates between the two
6827 methods in each case (midlatitude and polar) is a result of the differences in fractional
6828 release values. In the WMO (2007) case, the release factors are fixed values, while the
6829 release factors in the Newman *et al.* (2006) curves are mean age dependent. Note that the
6830 Newman *et al.* (2006) release factors at midlatitude are generally smaller for the three-
6831 year mean age than the values used in WMO (2007), leading to an earlier EESC recovery
6832 date. In contrast, the Newman *et al.* (2006) release factors at the pole for the six-year
6833 mean age are larger than the WMO (2007) values, resulting in a later EESC recovery
6834 date.
6835
6836 Newman *et al.* (2006) raised the issue on the uncertainty on predicting the EESC
6837 recovery date associated with the choice of mean age and release factors to represent
6838 midlatitude of polar conditions. While the use of different mean ages would change the
6839 absolute timing of the recovery for baseline case and other test cases, we are reasonably
6840 confident that it would not change the conclusion about the relative effects of different
6841 test cases.
6842

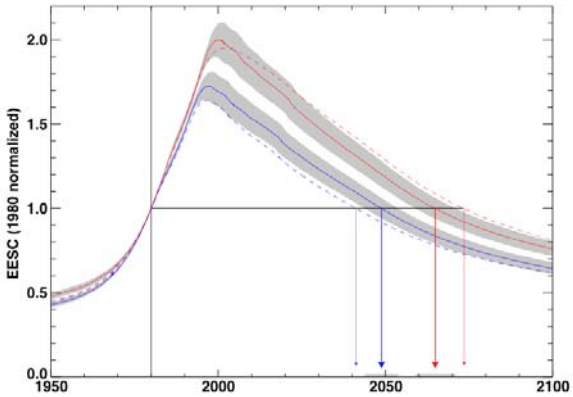

Figure 5.9 Comparison of EESC values calculated using a lag time and fixed fractional released values (dashed) *vs.* those calculated using a mean age with an age spectrum and fractional release values parameterized as functions of mean age (solid). The blue curves are for midlatitude with a mean age and lag time of three years. The curves for the polar region are in red calculated with a mean age and lag time of six years.

5.5.3 Time Series of Radiative Forcing

To adhere to the requirements of the Montreal Protocol, several courses of action have been adopted, including not-in-kind replacements of ODSs and changes in operations that reduce emissions. Applications that previously used CFCs are now performed with CFC replacements, HCFCs and HFCs, with HFCs likely to play a larger role in the future as HCFCs are phased out by the Montreal Protocol. Because HFCs contain no chlorine, bromine, or iodine, they do not destroy stratospheric ozone and therefore are not considered in WMO (2007). Furthermore, because future HFC emissions and production are not regulated by the Montreal Protocol, as are HCFCs, future projections of HFC concentrations are generally much more uncertain than those of ODSs and are heavily dependent on future economic growth assumptions and policy decisions. The forcing from HFCs will be included here as part of the discussion. However, it should be pointed out that the replacement strategy may also involve changes in other greenhouse gas

emissions associated with the life cycle analyses (IPCC/TEAP, 2005). The change in forcing associated with those greenhouse gases is not included in the discussion.

Once the mixing ratio time series has been determined, it is a simple matter to estimate the future direct radiative forcing due to the various compound groups from the radiative efficiencies of each ODS (WMO, 2007). This forcing time series, calculated by scaling the mixing ratio time series by the radiative forcing efficiencies of the particular ODSs is shown on the right-hand side of Figure 5.6. The continued importance of the CFCs, along with the importance of the HCFCs is perhaps the most striking features of this figure. The forcing contributions of the halons and CH_3Br are small because of their small atmospheric mixing ratios. The effect of the bromocarbons on ozone depletion is enhanced because of the higher efficiency of bromine compared to chlorine to destroy ozone; such a chemically-caused enhancement does not apply to radiative forcing. The potential reduction in forcing due to the elimination of future production and emission is shown for CFCs, HCFCs, halons, and CH_3Br in the lower 4 panels. It is evident that elimination of future HCFC emission has the large effect on radiative forcing of the ODSs among the test cases considered here. This peak forcing reduction of almost 0.07 W per m^2 represents slightly less than 5% of the CO_2 radiative forcing in 2000 and less than half of the N_2O radiative forcing in 2000.

The forcing of the HFCs, generally used as replacements for the ODSs are included in the figure as the orange shaded region for the SRES (Nakićenović *et al.*, 2000) A1B scenarios. The line within the orange region represents the alternate forcing of the HFCs in the B1

SRES scenario. Atmospheric observations suggest that the 2000 forcing due to the HFCs is slightly larger than that estimated by the SRES scenarios, primarily due to the higher abundances of HFC-23 observed.

The indirect forcing from the ODSs is shown in Figure 5.6 as the red hatched region. It represents an uncertainty range of ±100% around the best estimate, taken from IPCC (2007). The large uncertainty is associated with the simplifying assumption of a linear relationship between ozone depletion and EESC above the 1980 threshold. The best estimate suggests that ozone depletion offsets about one-sixth of the total ODS forcing around 2000. This figure also shows that the indirect forcing will gradually diminish in the coming decades returning to near 0 around 2050. This is the result of the assumption that the EESC value in 1980 represents a threshold, below which ozone depletion does not respond to changing EESC levels. While such a picture is likely imperfect, global ozone data do suggest that the response of ozone to EESC did change around this time. Finally, there have been studies suggesting that ozone radiative forcing may lead to a substantially different temperature response than does the same radiative forcing change from CO_2 [Joshi *et al.*, 2003 and references therein] Radiative forcing associated with ozone increase from climate changes is not included in this figure.

5.6 UNITED STATES CONTRIBUTIONS TO EESC AND RADIATIVE FORCING

Because of the long-lived nature of the ODSs, midlatitude EESC and the radiative forcing arising from emissions of these compounds should be thought of as global quantities.

This allows the contribution to midlatitude EESC and global radiative forcing to be apportioned to individual countries if their emissions are accurately known. As discussed in Chapter 2 in this report, ODS production and consumption amounts for the U.S. are reported to UNEP as required by the Montreal Protocol (UNEP, 2007). Data are also compiled by the Alternative Fluorocarbons Environmental Acceptability Study (AFEAS, 2007) for certain ODSs and for HFC-134a, although the amount reported to AFEAS has represented a smaller fraction of global production in the last decade or so when compared with the UNEP data. A discussion of the comparison of the data from these two compilations with observed atmospheric mixing ratio observations is provided in Chapter 2. Also in response to a requirement of being a signatory to the Montreal Protocol, the U.S. Environmental Protection Agency (EPA) uses a vintaging model to estimate annual emissions from the estimated production and consumption values after 1985. Chapter 2 discusses the results from the EPA's vintaging model through the past and the assumptions made to estimate United States emissions prior to 1984. Specifically, the pre-1975 CFC emissions were assumed to be between one-third and two-thirds of the global emissions. The United States emission for a CFC in 1985 as a percentage of global emission is assumed to be the averaged percentage emission between 1985 and 1990. The assumption is that the post-1985 emissions have an uncertainty of ±33%. The emissions between 1975 and 1984 are obtained from interpolation between the 1975 and 1985 values. Here, we use these assumptions along with the EPA's projections to estimate future levels of source gases attributable to the U.S. and their contributions to both EESC and radiative forcing.

5.6.1 Contribution to EESC

Given the assumptions used to derive historical United States emissions, it is useful to note that the EESC in 2030 is 2400 ppt, with about one-third from the natural CH_3Cl and CH_3Br. For the remaining two-thirds attributed to man-made emissions, ~15% is due to emissions prior to 1975, ~20% due to emissions between 1975 and 1984. The contributions from United States emissions to the loading in 2030 due to man-made emissions are 4.5-9% from United States pre-1975 emissions, 2-9% from United States emissions between 1975 and 1984, and 9-19% from United States emissions after 1985. Summing the contributions, we estimate that the midlatitude anthropogenic EESC amount resulting from United States emissions represents about 15-37% of the EESC amount resulting from all global emissions.

5.6.2 Contribution to Radiative Forcing

For radiative forcing, we estimate the United States emissions will contribute approximately 19-41% of the global forcing by 2030. The lower end of this range remains roughly constant until 2030, while the upper end gradually declines from about 47% in 2010. As was done for the previous EESC contribution results, these forcing estimates are calculated only considering anthropogenic emissions. Future United States PFC and SF6 emissions, which contribute very little to future radiative forcing (<10-5 W per m^2 through 2030), are estimated from the U.S. EPA vintaging model, while the future global abundances of these compounds are taken from the A1B and B1 SRES scenarios (SRES ref). If global PFCs and SF6 were not considered in the radiative forcing

calculation, United States emissions are projected to contribute about 20-43% of global radiative forcing in 2030.

5.6.3 Options for United States ODS Banks

The accessible and total bank size estimates for United States equipment and applications in 2005 are compared to global bank estimates from WMO (2007) in Table 5.3. Additional reduction cases are shown in Table 5.3 that quantify the importance of the recovery and destruction of United States total banks and United States accessible banks. The U.S. EPA has defined "accessible" banks as the quantity of ODSs that is contained in equipment (*i.e.*, fire protection equipment and refrigeration/air conditioning systems). Furthermore, it is assumed that the amount of ODS recoverable from this equipment is equal to the full equipment charge minus the average annual loss rate from leakage and servicing. It is possible that some of the non-accessible banks could be recovered and destroyed with the proper financial incentives and/or technological advances. Table 5.3 shows that the Halon 1301 and HCFC-22 United States accessible banks are the most substantial in terms of contributing to potential future integrated EESC reductions If the total United States banks are considered, CFC-11, HCFC-141b, CFC-12, HCFC-22, and Halon 1301 banks are most important. The calculations for the United States halon banks do not include stockpiles, and so these calculations should be considered to be an underestimate of the full possible benefit of recovering and destroying their banks.

Table 5.3 Comparison of global and United States bank elimination projections in terms of integrated EESC and ODS recovery time. The global test cases are taken from WMO (2007) and consider elimination of the global bank in 2007. U.S. cases assume elimination of the full U.S. bank, or the accessible U.S. bank in 2009.

Scenario	Percent Difference in integrated EESC relative to baseline scenario for the midlatitude case		Year (x) when EESC is expected to drop below 1980 value	
	Midlatitude			Antarctic vortex
	$\int_{1980}^{x} EESC\,dt$	$\int_{2007}^{x} EESC\,dt$		
Scenarios				
A1: Baseline scenario			2048.9	2065.1
Cases of full recovery of the 2007 banks[b] of:				
B0: All ODS (global)	-12.9	-27.8	2040.8	2056.7
CFCs (global)	-5.2	-11.3	2045.1	2060.4
CFC-11 (U.S., accessible)	-0.0[a]	-0.0[a]	2048.1	2064.1
CFC-12 (U.S., accessible)	-0.0[a]	-0.1	2048.9	2065.0
CFC-11 (U.S., total)	-1.1	-2.3	2048.1	2064.1
CFC-12 (U.S., total)	-0.3	-0.7	2048.7	2064.8
Halons (global)	-6.7	-14.3	2045.7	2062.0
Halon 1211 (U.S., accessible)	-0.1	-0.2	2048.9	2065.0
Halon 1301 (U.S., accessible)	-0.3	-0.6	2048.7	2064.8
Halon 1211 (U.S., total)	-0.1	-0.2	2048.9	2065.0
Halon 1301 (U.S., total)	-0.3	-0.6	2048.7	2064.8
HCFCs (global)	-1.9	-4.1	2048.4	2064.8
HCFC-22 (U.S., accessible)	-0.3	-0.6	2048.8	2065.0
HCFC-22 (U.S., total)	-0.3	-0.7	2048.8	2065.0
HCFC-141b (U.S., total)	-0.4	-0.8	2048.8	2065.0
HCFC-142b (U.S., total)	-0.1	-0.1	2048.9	2065.0

[a] Values reported as -0.0 are smaller than 0.05% in magnitude.

[b] Accessible bank values for HCFC-141b and HCFC-142b are not provided because the U.S. EPA estimates a zero accessible bank size for these compounds.

CHAPTER 5 REFERENCES

Daniel, J.S., S. Solomon, and D.L. Albritton, 1995: On the evaluation of halocarbon radiative forcing and global warming potentials. *Journal of Geophysical Research,* **100(D1)**, 1271-1285.

Eyring, V., N. Butchart, D. W. Waugh, H. Akiyoshi, J. Austin, S. Bekki, G. E. Bodeker, B. A. Boville, C. Brühl, M. P. Chipperfield, E. Cordero, M. Dameris, M. Deushi, V. E. Fioletov, S. M. Frith, R. R. Garcia, A. Gettelman, M. A. Giorgetta, V. Grewe, L. Jourdain, D. E. Kinnison, E. Mancini, E. Manzini, M. Marchand, D. R. Marsh, T. Nagashima, P. A. Newman, J. E. Nielsen, S. Pawson, G. Pitari, D. A. Plummer, E. Rozanov, M. Schraner, T. G. Shepherd, K. Shibata, R. S. Stolarski, H. Struthers, W. Tian, and M. Yoshiki, 2006: Assessment of temperature, trace species and ozone in chemistry-climate model simulations of the recent past, *Journal of Geophysical Res*earch, **111**, D22308, doi:10.1029/2006JD007327.

Eyring, V., D.W. Waugh, G.E. Bodeker, E. Cordero, H. Akiyoshi, J. Austin, S.R. Beagley, B.A. Boville, P. Braesicke, C. Brühl, N. Butchart, M.P. Chipperfield, M. Dameris, R. Deckert, M. Deushi, S.M. Frith, R.R. Garcia, A. Gettelman, M.A. Giorgetta, D.E. Kinnison, E. Mancini, E. Manzini, D.R. Marsh, S. Matthes, T. Nagashima, P.A. Newman, J.E. Nielsen, S. Pawson, G. Pitari, D.A. Plummer, E. Rozanov, M. Schraner, J.F. Scinocc, K. Semeniuk, T.G. Shepherd, K. Shibata, B. Steil, R.S. Stolarski, W. Tian, and M. Yoshiki, 2007: Multimodel projections of stratospheric ozone in the 21st century, *Journal of Geophysical Research,* **112**, D16303, doi:10.1029/2006JD008332.

Hadjinicolaou, P., J.A. Pyle, and N.R.P. Harris, 2005: The recent turnaround in stratospheric ozone over northern middle latitudes: A dynamical modeling perspective, *Geophysical Research Letters*, **32**, L12821, doi:10.1029/2005GL022476.

IPCC (Intergovernmental Panel on Climate Change), 1999: *Aviation and the Global Atmosphere*, Special Report of Working Group I and Working Group III of IPCC,

edited by J.E. Penner, D.H. Lister, D.J. Griggs, D.J. Dokken, and M. McFarland, 373 pp., Cambridge University Press, Cambridge, U.K.

IPCC (Intergovernmental Panel on Climate Change), 2001: *Climate Change 2001: The Scientific Basis: Contribution of Working Group I to the Third Assessment Report of the Intergovernmental Panel on Climate Change*, edited by J.T. Houghton, Y. Ding, D.J. Griggs, M. Noguer, P.J. van der Linden, X. Dai, K. Maskell, and C.A. Johnson, 881 pp., Cambridge University Press, Cambridge, U.K.

IPCC (Intergovernmental Panel on Climate Change), 2007: *Climate Change 2007: The Physical Science Basis. Contribution of Working Group I to the Fourth Assessment Report of the Intergovernmental Panel on Climate Change*, edited by S. Solomon, D. Qin, M. Manning, Z. Chen, M. Marquis, K.B. Averyt, M. Tignor, and H.L. Miller, 996 pp., Cambridge University Press, United Kingdom and New York, NY, USA.

IPCC/TEAP (Intergovernmental Panel on Climate Change / Technology and Economic Assessment Panel), 2005: *IPCC/TEAP Special Report on Safeguarding the Ozone Layer and the Global Climate System: Issues Related to Hydrofluorocarbons and Perfluorocarbons*, edited by B. Metz, L. Kuijpers, S. Solomon, S.O. Andersen, O. Davidson, J. Pons, D. de Jager, T. Kestin, M. Manning, and L. Meyer, 478 pp., Cambridge University Press, New York.

Joshi, M., K. Shine, M. Ponater, N. Stuber, R. Sausen, and L. Li, 2003: A comparison of climate response to different radiative forcings in three general circulation models: Towards an improved metric of climate change. *Climate Dynamics*, **20**, 843-854.

Nakićenović, N., J. Alcamo, G. Davis, B. de Vries, J. Fenhann, *et al.*, 2000: Special Report on Emissions Scenarios (SRES), A Special Report of Working Group III of the Intergovernmental Panel on Climate Change, Cambridge University Press, Cambridge, UK.

Newman, P.A., E.R. Nash, S.R. Kawa, S.A. Montzka, and S.M. Schauffler, 2006: When

will the Antarctic ozone hole recover?, *Geophys. Res. Lett., 33,* L12814, doi: 10.1029/2005GL025232.

UNEP (United Nations Environment Programme), 2007: Ozone Secretariat ODS production and consumption data tables on the web at <http://ozone.unep.org/Data_Reporting/>.

UNEP/TEAP (United Nations Environment Programme/Technology and Economic Assessment Panel), 2007: Report of the Task Force Response on HCFC Issues and Emissions Reduction Benefits Arising from Earlier HCFC Phase-Out and Other Practical Measures, 132 pp.

WMO (World Meteorological Organization), 1995: *Scientific Assessment of Ozone Depletion: 1994, Global Ozone Research and Monitoring Project–Report No. 37*, Geneva, Switzerland.

WMO (World Meteorological Organization), 1999: *Scientific Assessment of Ozone Depletion: 1998, Global Ozone Research and Monitoring Project–Report No. 44*, Geneva, Switzerland.

WMO (World Meteorological Organization), 2003: *Scientific Assessment of Ozone Depletion: 2002, Global Ozone Research and Monitoring Project–Report No. 47*, Geneva, Switzerland.

WMO (World Meteorological Organization), 2007: *Scientific Assessment of Ozone Depletion: 2006, Global Ozone Research and Monitoring Project–Report No. 50*, Geneva, Switzerland.

Yang, E.S., D.M. Cunnold, R.J. Salawitch, M.P. McCormick, J. Russell III, J.M. Zawodny, S. Oltmans, and M.J. Newchurch, 2006: Attribution of recovery in lower-stratospheric ozone. *Journal of Geophysical Research*, **111**, D17309, doi:10.1029/2005JD006371.